Lumped-intermediates analysis in the photooxidation of Rhodamine 6G in the H₂O₂/UV system

Amaia Menendez*,†, Jose I. Lombraña, and Ana de Luis***

*Department of Chemical Engineering and Environment, University School of Mining and Civil Technical Engineering,
University of the Basque Country, Colina Beurko, s/n. 48902, Barakaldo (Bizkaia), Spain
**Department of Chemical Engineering, University of the Basque Country, P.O. Box 644, 48080, Spain

Abstract−The combination of H₂O₂ with UV radiation was applied to study the degradation of Rhodamine 6G dye (Rh-6G). The lumped kinetic model proposed in this work is a reaction-system scheme to describe the degradation of dye using lumps of intermediate compounds grouped by their chemical and colorimetric behavior. Rate constants obtained by application of the model were shown to predict the progress of dye oxidation. The effects of pH and oxidant dosage on these rate constants were also analyzed. Finally, photodecoloration was studied considering the absorption at 528 nm (the maximum absorption wavelength of the dye) as the sum of all compounds absorbing at this wavelength: Rhodamine itself and the colored intermediates produced.

Key words: Lumped Kinetic Model, H₂O₂/UV, Rhodamine 6G, Decoloration, Dye

INTRODUCTION

Advanced oxidation processes (AOPs) are able to degrade pollutants into harmless substances, making them one of the major technological resources for the treatment of liquid effluents, air and sludge pollutants. These processes are especially attractive for the treatment of polluted water because they can mineralize the initial contaminant to the ultimate degree, i.e., to carbon dioxide, water and corresponding salts [1]. Nevertheless, the possibility of the formation of intermediates with greater toxicity than the initial pollutant requires the study of each particular case [2].

The present work focused on the application of hydrogen peroxide in combination with ultraviolet light in water containing low concentrations of dyes. The oxidative effect of the H₂O₂/UV system is based on the high reactivity of ·OH generated by the photolysis of H₂O₂. The quantum yield of H₂O₂ is unity at 254 nm, producing two ·OH radicals per molecule of H₂O₂. In addition, some pollutants are also directly photolyzed, increasing the efficiency of the oxidation process.

A kinetic model is essential for the analysis and following design of wastewater treatments in similar real-world situations. In this study, not only the primary degradation of Rhodamine 6G (Rh-6G) but also the consequent degradation stages up to mineralisation were analyzed. Previous studies have defined simple series reaction models to describe the degradation of well-defined compounds by an H₂O₂/UV system [3,4] and others have proposed lumped kinetic models applied to a wet-oxidation process [5-7]. In our previous work, a lumped kinetic model for the degradation of a linear alkylbenzenesulphonate (LAS) surfactant in an H₂O₂/UV system was proposed [8]. That model was based on prior observations and assumed the formation of intermediate lumps with different absorp-

tion behaviors at the two wavelengths which are characteristic of the initial compound and which have common chemical structures.

In another study on the specific case of dye removal and water decoloration, a basic lumped kinetic model was proposed [9]. In the present work, an improvement of the preceding model is proposed; more lumps with higher complicity and consequently more paths were considered. In the lumped kinetic model proposed here, three intermediate degradation stages before complete degradation were assumed; each consists of a lump of compounds grouped by their stage of mineralization and subsequent colorimetric behavior.

MATERIALS AND METHODS

1. Chemicals and Analysis

One of the most important families of compounds derived from xanthene is that of the Rhodamine compounds, particularly Rhodamine 6G (Rh-6G), also widely known as Basic Red 1. This basic dye (molecular structure shown in Fig. 1) was taken as a model dye for this study. The Rhodamine 6G (Rh-6G) was supplied by Sun Chemical (Asua-Vizcaya, Spain) and used for the preparation of the synthetic model dye wastewaters. Hydrogen peroxide (30 wt%) was supplied by PANREAC.
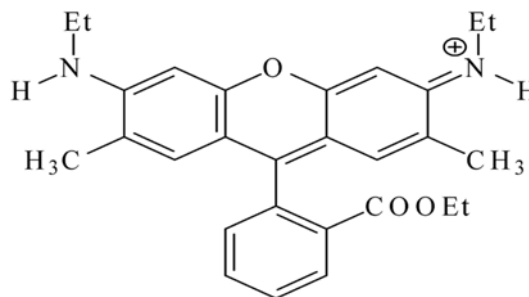

Fig. 1. Molecular structure of Rhodamine 6G (Rh-6G).

†To whom correspondence should be addressed.
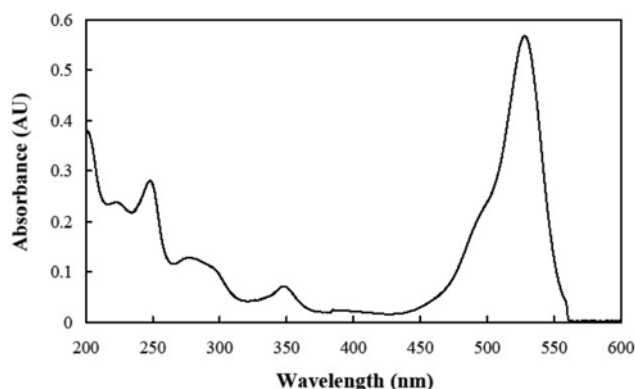E-mail: amaia.menendez@ehu.es
*Relative

Fig. 2. Absorption spectrum of Rh-6G dye in water at unadjusted pH.

Fig. 3. Calibration curve of Rhodamine 6G Absorption at 528 nm in water at natural pH.

The Rhodamine 6G was analyzed by means of the Alliance 2695 HPLC WATERS apparatus, with a UV/VIS WATERS 2487 detecting system (528 nm). A chromatographic column (Waters Spherisorb, 4.6×150 mm, 5 μm in diameter) filled with ODS2 material was used, along with a Tr-C-160Kl precolumn also filled with ODS. An 80/20 methanol/water solution was used as the eluent, buffered to pH 3 with a phosphate/phosphoric acid solution using a carrier flow controlled at around 1.0 mL min⁻¹.

This study analyzed not only Rhodamine but also the color measured by the absorption at 528 nm (the maximum absorption wavelength of Rh-6G, λ_{max}, see Fig. 2). This measure was related to the concentration of colored intermediates that, during the first stages of the degradation process, maintained the absorption capacity of the chromophore group of Rh-6G. Measurements were performed on a Perkin Elmer Lambda 10 UV/VIS spectrophotometer using standard colorimetric methods [10]. Total organic carbon (TOC) was measured in a TOC-5000A Shimadzu analyzer. The reaction pH was determined using a pHRocon 18 CRISON pH meter pre calibrated with buffered solutions at pH 4.00 and 7.02.

2. Photoreactor

Oxidation experiments were carried out in a 1-L stirred reactor vessel with measuring elements for pH and temperature. A low-pressure mercury lamp (Heraeus, mod. TNN 15/32; 254 nm, 19 W) mounted inside a concentric quartz tube was placed axially and centered in the vessel. Samples were taken at regular time intervals noting the pH values. Later, the samples were analyzed by UV/VIS spectrophotometry, HPLC and TOC. Homogenization of the solution was obtained by magnetic stirring in the reactor and the reaction was carried out at room temperature.

RESULTS AND DISCUSSION

1. Lumps of Intermediates

Numerous authors have studied decoloration of water through the absorbance at the maximum wavelength of the dye [11-14], and others have attributed the absorption at the maximum only to the dye [15-17]. In some cases [18], when removal of dye (and color) was achieved by absorption it is valid to consider absorbance at the maximum wavelength of the dye as the dye concentration. However, Elmorsi et al. [19] considered the absorbance not only by the dye but also by the intermediates produced without independently
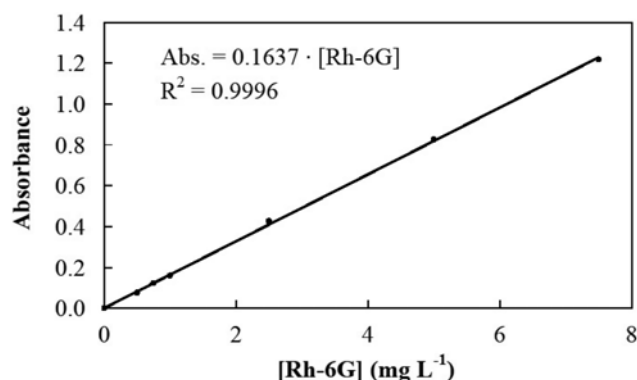
analyzing both. Nevertheless, recent works have proved that the rate of degradation of the dye (analyzed by means of HPLC) does not match the absorbance-decrease rate which would be justified by the presence of other colored intermediates with chromophore groups similar to that of Rh-6G absorbing at its maximum absorbance wave length (λ_{max}=528 nm) [9]. For this reason, in this work two processes were considered individually: dye elimination and water decoloration. Intermediates were identified and quantified through their absorbance at 528 nm, grouping them in one lump of intermediates that retained the characteristic chromophore group absorbing at the wavelength of the original dye (528 nm). This intermediate lump, called colored intermediates (CI), was quantified in terms of its colorimetric behavior through the balance of absorbance:

$$[Color]=[Rh\text{-}6G]+[CI] \tag{1}$$

In Eq. (1), all three terms are expressed as equivalent mg/L of Rhodamine, defined as the light absorbed by one mg/L of Rhodamine following the calibration curve of Fig. 3. While [Rh-6G] was obtained by HPLC analysis, [Color] was obtained by colorimetric analysis and expressed in equivalent mg/L of Rhodamine. In this work, reactions were conducted at pH 3 with a phosphate/phosphoric acid solution as a buffer to develop a lumped kinetic model, and the model validity was then studied when the reaction was carried out at natural (*unadjusted*) pH.

The UV/H_2O_2 process was also characterized in terms of by-product formation. This is an important task in groundwater remediation because it must be assessed whether or not the treatment employed leads to the formation of toxic compounds.

2. Lumped Kinetic Model

This study focused on the modelling of Rhodamine 6G oxidation with the further study of color removal based on the lumped kinetic model. The proposed model is an improvement on an earlier two-stage model based solely on colored intermediates derived from Rhodamine 6G [9]. The new lumped kinetic model describes oxidation up to complete degradation by modelling a reaction system in which, apart from colored intermediates absorbing at 528 nm (CI), two new lumps of colorless intermediates are considered based on the complexity of their structures. Both new lumps were needed to describe the stages of mineralization of the process and to achieve a good fitting of experimental data. The lump CI was considered to come directly from Rhodamine 6G:

$$Rh\text{-}6G \xrightarrow{k_1} CI \qquad (2)$$

This lump, consisting of colored intermediates, yields colorless intermediates (CLI) that do not contribute to color:

$$CI \xrightarrow{k_2} CLI \qquad (3)$$

Thus far the kinetic model is identical with the classic series model used previously [9], in which the lump of colorless compounds was assumed to be the final product of the reaction mechanisms and was therefore called CLC (colorless compounds) rather than CLI (colorless intermediates) as in this new model. The innovation of the present model over the previous one is that the CLI is understood as a lump of intermediates, whereas before the reaction was modelled as ending with these colorless compounds. Nevertheless, it seems logical that Rh-6G could also yield CLI, which is assumed to have a complex structure similar to Rhodamine 6G, from which its components are derived in a 1 : 1 stoichiometry as a result of the initial oxidative attacks on the chromophore functions of both Rh-6G and CI.

$$Rh\text{-}6G \xrightarrow{k_3} CLI \qquad (4)$$
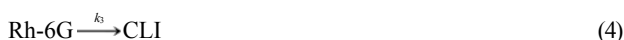
Moreover, the lump of complex intermediates CLI gives rise to intermediate compounds with a simpler structure (SI) due to the degradation process, which also do not contribute to color in the medium. This lump SI was included in the new model to better fit the experimental data and could be considered the initial step of the last stage before becoming mineralized matter (MM), i.e., carbon dioxide and water.

$$CLI \xrightarrow{k_4} SI \qquad (5)$$

$$SI \xrightarrow{k_5} MM \qquad (6)$$
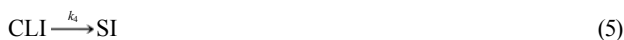
Summarizing, the lumped kinetic model proposed here is the combination of two different models: the general lumped kinetic model [20] used in the transformation of Rh-6G dye to the CLI lump and the classic series lumped kinetic model used to explain the subsequent mineralization of CLI. Both lumped kinetic models have also been used in other works [21], but the difference is that here both were joined to fit the experimental data.

In this scheme of reactions from (2) to (6), color is the sum of Rhodamine and the CI intermediate lump. Fig. 4 shows the evolution of experimental concentrations (symbols) of the compounds
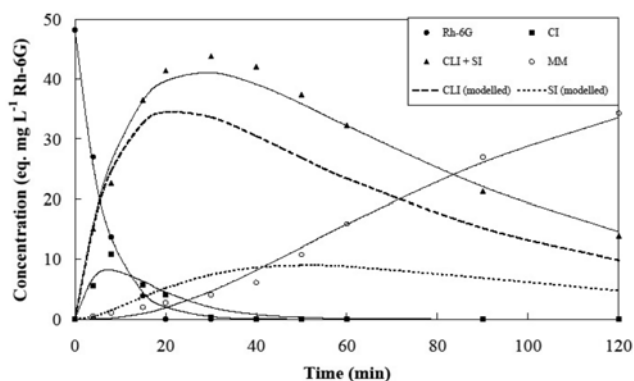

Fig. 4. Modelled and experimental kinetic data for 6.3 mmol H_2O_2/ L at pH 3.

and lumps of intermediates described above. Supposing that each of the five reactions considered follows first-order kinetics, the reaction-rate equations for the lumps involved can be expressed as follows:

$$-\frac{d[Rh\text{-}6G]}{dt} = (k_1 + k_3)[Rh\text{-}6G] \qquad (7)$$

$$\frac{d[CI]}{dt} = k_1[Rh\text{-}6G] - k_2[CI] \qquad (8)$$

$$\frac{d[CLI]}{dt} = k_3[Rh\text{-}6G] + k_2[CI] - k_4[CLI] \qquad (9)$$

$$\frac{d[SI]}{dt} = k_4[CLI] - k_5[SI] \qquad (10)$$

$$\frac{d[MM]}{dt} = k_5[SI] \qquad (11)$$

From Eq. (7), it is deduced that the rate constant for the disappearance of Rhodamine is expressed by the sum of the first-order rate constants k_1 and k_3:

$$k_{Rh\text{-}6G} = k_1 + k_3 \qquad (12)$$

To solve this system of equations, the concentrations of lumps CI and MM are determined experimentally. The concentration of lump CI is calculated from Eq. (1) as the difference between the absorbance at 528 nm of the sample and that of the remaining Rhodamine 6G as determined by HPLC. This difference refers only to CI compounds and is expressed in equivalent mg/L of Rhodamine using the corresponding absorbance-concentration relationship at 528 nm.

Once the concentration of MM is known by TOC analysis, the mass balance of Eq. (13) is applied in terms of equivalent mg/L of Rhodamine. Here, the concentration of each lump equates to the amount of initial Rhodamine yielding such a lump.

$$[Rh\text{-}6G]_0 = [Rh\text{-}6G] + [CI] + [CLI] + [SI] + [MM] \qquad (13)$$

The concentration of each compound and intermediate lump was calculated according to the proposed model by solving Eqs. (7)-(12) and (13) in Matlab 6.5. The solution provided the rate constants yielding the minimum least squares differences between the experimental and modelled values of Rh-6G, CI and MM. Thus, the rate constants from k_1 to k_5 were obtained. Additionally, the concentration values predicted by the model for Rh-6G, CI, MM and the sum of CLI and SI obtained from Eq. (13) were fitted to the corresponding experimental data.

Oxidation experiments were carried out on a 50 mg/L Rh-6G solution for 2 h at pH 3, varying oxidant dosage from 0 to 400 mol H_2O_2/mol Rh-6G (0 to 41.7 mmol H_2O_2/L). As an example, the fit obtained between modelled results of lump concentrations (lines) and experimental ones (symbols) is shown in Fig. 4 for an oxidant dosage of 60 (6.3 mmol H_2O_2/L) and pH 3. These lumps of intermediate compounds reached a maximum level of formation and then slowly disappeared. This indicates that a certain degree of organic mineralization can be also obtained by UV/H_2O_2 oxidation.

The rate constants obtained by applying the model are listed in Table 1 for all oxidant dosages studied at pH 3. The rate constant for Rhodamine removal is the sum of the first-order rate constants k_1 and k_3 according to Eq. (12). Focusing on kinetics, the rate-limiting

**Table 1. Rate constants obtained from the lumped kinetic model at pH 3**

D (mol H₂O₂/mol Rh-6G)	0	20	60	120	400
k_1 (min⁻¹)	0.0084	0.0557	0.0594	0.0788	0.0823
k_2 (min⁻¹)	0.0197	0.0657	0.1012	0.1136	0.2323
k_3 (min⁻¹)	0.0203	0.0549	0.0983	0.1274	0.2346
k_4 (min⁻¹)	0.0012	0.0069	0.0146	0.0160	0.0111
k_5 (min⁻¹)	0.0344	0.0483	0.0431	0.0994	0.2647
$k_{Rh\text{-}6G}$ (min⁻¹)	0.0287	0.1105	0.1577	0.2062	0.3169
$R^2_{Rh\text{-}6G}$	0.9964	0.9967	0.9977	0.9975	0.9968
R^2_{CI}	0.9313	0.9844	0.9189	0.8919	0.9792
R^2_{MM}	0.9523	0.9963	0.9926	0.9897	0.9878
$\overline{R}^2$	0.9600	0.9925	0.9697	0.9597	0.9879
k_d (min⁻¹)	0.0200	0.0631	0.1005	0.1158	0.2637
R^2_d	1.0000	0.9992	1.000	0.9997	0.9992

step is clearly the step from the lump of complex intermediates CLI to the lump of intermediates with less complex molecular structures, SI.

3. Model Verification

The standard deviation of the predicted model concentrations for Rh-6G, CI and MM with respect to the experimental concentrations, defined as the square root of the variance, was calculated in all cases. Table 1 shows the standard deviation of the modelled concentration values obtained after the fitting process was solved in Matlab for the three compounds analyzed; the mean values of the lump standard deviations and the determination coefficient R^2 are also shown for each experiment. The *significance of the rate constants predicted by the lumped kinetic model was evaluated using the graph representing the percentage of each in an experiment conducted to pH 3 over two hours but with different dosages of oxidant (see Fig. 5). From this representation, small values of the rate constant k_4 were identified in all cases, indicating that the step corresponding to that rate constant was the limiting one for the whole process of Rhodamine mineralization.

This work is focused on water decoloration so the *significance of the rate constants predicted by the lumped kinetic model for achiev-
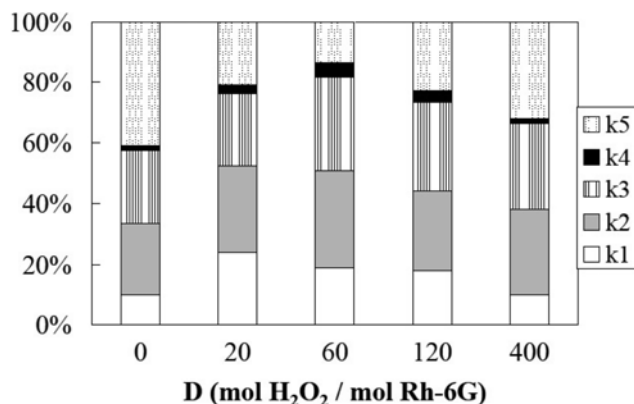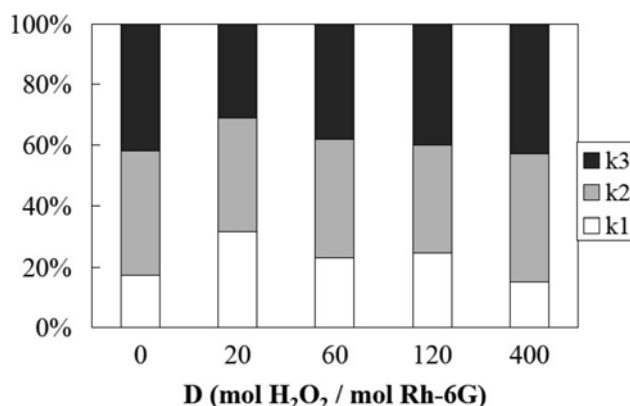
Fig. 6. *Significance of model rate constants for decoloration of water at pH 3.

ing decoloration was also evaluated by calculating the percentage contribution of each to decoloration in an experiment conducted at pH 3 over two hours at different dosages of H₂O₂. In Fig. 6, three rate constants were considered: k_1 and k_3, both corresponding to dye elimination in reactions (2) and (4), respectively, and k_2 for the removal of the colored-intermediates lump in reaction (3). In the case of the decoloration process, rate constants k_2 and k_3 presented very similar values while the rate-limiting step was the one related to the conversion of Rhodamine dye to colored intermediates (k_1).

This consideration of the rate-limiting step for decoloration leads to the comparison of two parallel paths to achieve decoloration (arriving at the colorless-intermediate lump, CLI): on the one hand, Rhodamine is converted to CLI in the sum of two steps (reactions 2 and 3); on the other hand, dye is transformed in reaction (4) directly into CLI. In Fig. 7 both paths are represented showing that the path of the sum of reactions (2) and (3) (k_1+k_2) was significantly faster than that for reaction (4) (k_3). On the secondary axis the ratio of both paths (k_1+k_2)/k_3 is represented where the highest value was found for oxidant initial dosage D=20 mol H₂O₂/mol Rh-6G (2.1 mmol H₂O₂/L).

Additionally, the competitive reactions in Rhodamine removal, i.e., reactions (2) and (4), were analyzed to simplify the model to one of only two stages in series. This simplification seems justifiable if the rate constant k_3 is greater than k_1, which would obviate modelling the direct formation of the CI compounds from Rh-6G. The values obtained by the lumped kinetic model for rate constant

Fig. 5. *Significance of model rate constants for mineralization of Rh-6G at pH 3.
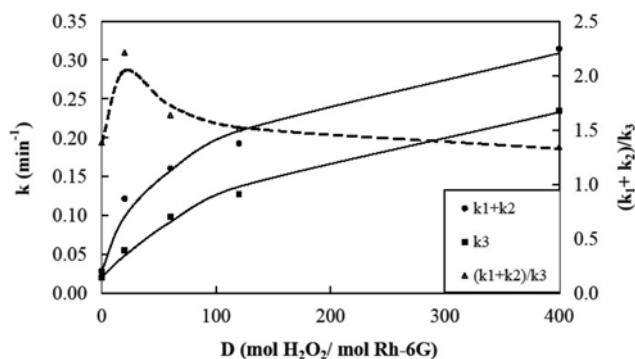
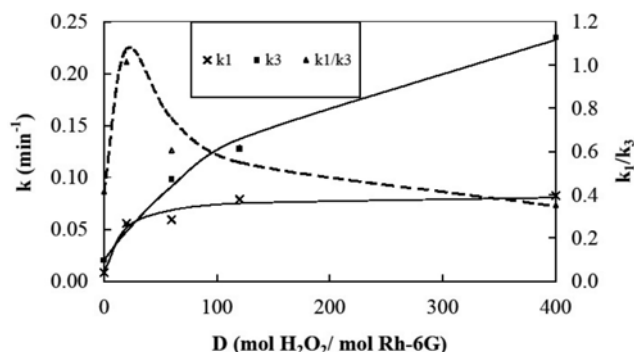**Fig. 7. Comparison of paths for the decoloration process at pH 3.**

Fig. 8. Comparison of paths for the dye-removal process at pH 3.

k_1 were from 35% to 60% of the value for k_3, except when k_1 reached the value of k_3 for an oxidant dosage of 20 mol H_2O_2/mol Rh-6G. The relative significance of the two parallel paths was analyzed by means of the relative variation of the rate constants governing the two primary degradation paths. Fig. 8 shows that the maximum of the k_1/k_3 ratio was at a value of 1 for a 2.1 mmol H_2O_2/L oxidant initial dosage (D=20 mol H_2O_2/mol Rh-6G).

Upon analyzing the values of the rate constants in Table 1, it seemed that such a simplification of the model was not possible, as k_3, although less important, can reach values similar to k_1 at intermediate oxidant dosages. Therefore, the two parallel degradation paths of Rh-6G dye must be considered: the one that gives rise to CI, which maintains the chromophore group and is governed by the rate constant k_1, and the other route, governed by the rate constant k_3, that gives rise to the formation of CLI with loss of the chromophore group.

4. Model Validation at Unadjusted pH

In the previous section, Rh-6G degradation at pH 3 was performed using a buffer solution to maintain constant pH throughout the process. For the sake of comparison, other experiments were conducted with no buffer and, consequently, a natural variation in pH was observed during the oxidation process. The change of pH usually gives rise to structural modifications of the dye [22], UV-visible absorbance properties and subsequent oxidation-rate effects [23].

As an example, the experimental data and those obtained after application of the model are shown for a reaction at natural pH, using a hydrogen peroxide dosage of 6.3 mmol H_2O_2/L (60 mol H_2O_2/mol Rh-6G). Fig. 9 shows how the modelled concentration profiles
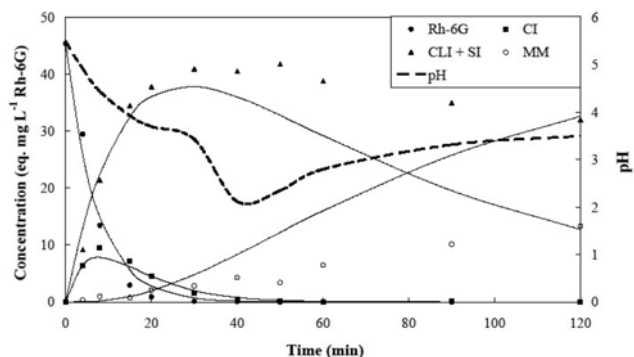

Fig. 9. Modelled and experimental kinetic data for 6.3 mmol H_2O_2/L at unadjusted pH.

fit the experimental data acceptably for the first 30 min of reaction but deviated later towards the end of the process. The pH profile is also shown in this figure. After the first 30 min, pH dropped sharply, and this can be related to the poor fit of the model thereafter. This deviation could be explained by the strong reduction in pH to about 2, which could implicate structural changes in the dye and intermediates [22]. This same abrupt pH drop was found for all the oxidant dosages analyzed.

Therefore, the model was able to predict reactions rapidly enough so that they were not affected by pH reduction. In Fig. 9, the fastest rates shown are those corresponding to the removal of Rhodamine and CI. In both cases, they had already disappeared by the time the drop in pH occurred. Consequently, this model could be used to predict fast color-elimination kinetics (Rh-6G and CI) with free pH evolution.

This particular behaviour at natural pH can be explained by the transformation of Rhodamine as the pH of the medium changes. Rh-6G is a molecule (see Fig. 1) with a cationic nature due to the presence of two amine groups [24]. These, depending on the pH, can form three different species as follows: $R^{2+} \leftrightarrow RH^+ \leftrightarrow RH_2$. The corresponding pK_a values for the first and second equilibria were obtained experimentally at 4.3 and 9, respectively. Due to the experimental conditions shown in Fig. 9, deviations occurred at pH around 4 that would enable the conversion of RH^+ to R^{2+}. In addition, the decrease of pH is usually associated with the oxidation of organic compounds to mineral acids, carbon dioxide and their acidic intermediates (Crittenden et al., 1999) [25]. Thus, although the primary degradation was not significantly affected by pH, it appears to have had a great significance on the subsequent oxidation, which explains the deviations observed after decoloration.

5. Effect of Oxidant Dosage on Rate Constants

A number of other researchers have previously studied the dependence of the rate constants for decoloration on the dosage of oxidant supplied [14,15,26-28]. As seen in Table 1, the rate constants calculated in solving the kinetic equations system of the model vary significantly with the hydrogen peroxide dosage (D).

A linear dependence of the rate constants with the dosage of oxidant has been reported [26], but in our case, the data were not well fitted by a linear expression. Other authors [27,28] have reported that the rate constants increased approximately linearly with the initial concentrations of hydrogen peroxide up to a threshold value in all cases, but the rate constants increased very slowly with further increases in H_2O_2 concentration up to this value.

These two effects of the amount of oxidant added at the beginning of the reaction on the rate constants could be valid for our data up to a low value of oxidant dosage; however, for extreme conditions (D=400 mol H_2O_2/mol Rh-6G) we observed that neither of the two findings above were relevant to our rate constants (Fig. 8). This was exactly the reason why runs were carried out at such extremely high dosages, i.e., to find the critical conditions that led us to a valid expression for a wide range of oxidant dosage.

In a previous work [29] an approach to find the dependence of the rate constants to the H_2O_2 dosage was made. In fact, in advanced oxidation processes such as the system studied in this work, there is a characteristic value for oxidant dosage normally called the *critical value*; an increase in H_2O_2 concentration leads to a faster degradation up to this critical value, but at higher dosages the degradation

Table 2. Parameters of the rate constants vs. oxidant dosage D

k	a (min⁻¹)	b (mol Rh-6G/mol H₂O₂·min)	c (mol Rh-6G/mol H₂O₂)	d (mol Rh-6G/mol H₂O₂)²	R^2
k_1	8.411 10^{-3}	5.055 10^{-3}	6.745 10^{-2}	-------	0.9666
k_2	1.971 10^{-2}	1.461 10^{-3}	4.509 10^{-3}	-------	0.9674
k_3	2.035 10^{-2}	1.507 10^{-3}	4.596 10^{-3}	-------	0.9936
k_4	1.249 10^{-3}	3.598 10^{-4}	7.384 10^{-3}	6.751 10^{-5}	0.9962
k_5	3.439 10^{-2}	5.647 10^{-4}	-------	-------	0.9860
$k_{Rh\text{-}6G}=k_1+k_3$	2.876 10^{-2}	3.502 10^{-3}	9.923 10^{-3}	-------	0.9846
k_d	2.000 10^{-2}	1.274 10^{-3}	2.793 10^{-3}	-------	0.9763
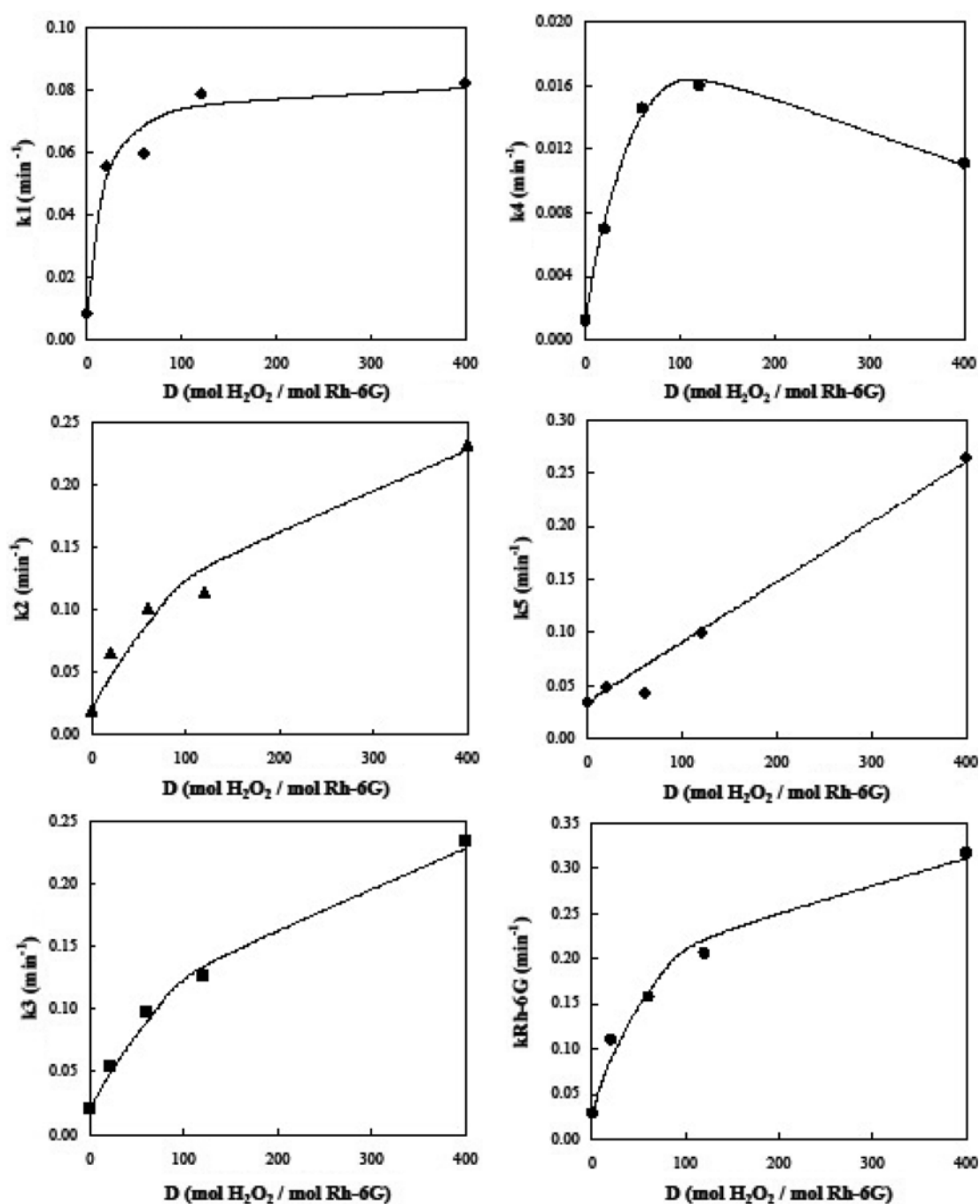
Fig. 10. Model rate constants and adjustments to Eq. (14) at pH 3.

process is slower [14,15]. For all rate constants this dependency follows Eq. (14) as proposed by Aleboyeh et al. [15], but only in the case of the rate constant of SI formation from CLI elimination are the four parameters (a, b, c and d) needed. Nevertheless, the other rate constants dispense with one or even two of the parameters of the expression in Eq. (14). Table 2 shows the equation coefficients for all the kinetics, along with the overall $k_{Rh\text{-}6G}$ (the sum of k_1 and k_3):

$$k = a + \frac{bD}{1 + cD + dD^2} \quad (14)$$

In Fig. 10, the values of the rate constants obtained by application of the lumped kinetic model are represented as dots while lines indicate the values satisfying Eq. (14).

6. Decoloration

Within the model scheme of kinetic reactions, the degradation of color was analyzed because of its visual impact. Color here is defined as the sum of compounds contributing to color, i.e., Rh-6G and the intermediate group CI. Consequently, the kinetic equation proposed to describe color removal is as follows:

$$-\frac{d[\text{Color}]}{dt} = -\frac{d[\text{Rh-6G}]}{dt} - \frac{d[\text{CI}]}{dt} = k_3[\text{Rh-6G}] + k_2[\text{CI}] \quad (16)$$

Once the concentration profiles of every intermediate group were obtained by applying the model, the color concentration was calculated as the sum of concentrations of Rh-6G and CI. The color kinetics thus calculated, the decoloration rate corresponding to the treatment of a 50 mg/L Rhodamine solution at pH 3, was fitted to a first-order kinetic equation:

$$-\frac{d[\text{Color}]}{dt} = k_d[\text{Color}] \quad (17)$$

Values for the decoloration rate constant (k_d) were obtained for the different oxidation dosages analyzed (Table 1). An equation of the form of Eq. (14) was found to fit acceptably the k_d rate constant at different D values. The corresponding coefficients are shown in Table 2.

7. Comparison of the Rh-6G- and Color-removal Processes

Finally, this section provides an analysis of the relationship between the two processes studied previously: the elimination of Rh-6G and decoloration. In most previous works, only one of these (usually decoloration) was studied, ignoring the other one. In this work, however, both processes were studied separately, enabling comparison between them. In this case, to contrast the processes, as in section 3.3 when the two paths for Rhodamine removal were compared, the rate constants were obtained for both processes and their ratio was determined. In Fig. 11, the symbols represent predictions obtained from the lumped kinetic model while the lines indicate data from the fitting to Eq. (14).

CONCLUSIONS

This study developed a lumped kinetic model to describe the different stages of Rhodamine 6G degradation up to complete mineralization. The kinetic model assumed five degradation paths with the inclusion of three lumps of intermediates. Data fitting for primary dye removal, decoloration and mineralization enabled the determination of rate constants for the five oxidative paths. The rate constants were used then to predict the concentrations of the different lumps and, in particular, to analyze the decoloration and mineralization at different oxidant dosages. It is clear that these are two different and independent processes that should not be confounded, as initial water color is due solely to the presence of the dye and as the reaction proceeds colored intermediates are produced that also contribute to the color. It is very important to consider dye and color removal independently during process optimization using the appropriate kinetic model. The model was validated at pH 3 for the whole oxidant range studied but only describes primary degradation acceptably at natural (unadjusted) pH because of the major pH changes appearing thereafter.

REFERENCES

1. H. Y. Shu and M. C. Chang, *Dyes Pigments*, **65**, 25 (2005).
2. P. B. L.Chang and T. M. Young, *Water Res.*, **34**, 2233 (2000).
3. A. de Luis, J. I. Lombrana, F. Varona and A. Menéndez, *Afinidad*, **57**, 439 (2000).
4. P. K. Malik and S. K. Sanyal, *Sep. Purif. Technol.*, **36**, 167 (2004).
5. J. Donlagic and J. Levec, *AIChE J.*, **45**, 2571 (1999).
6. Q. L. Zhang and K. T. Chuang, *AIChE J.*, **45**, 145 (1999).
7. S.Verenich and J. Kallas, *Environ. Sci. Technol.*, **36**, 3335 (2002).
8. A. Menendez, J. I. Lombrana and A. de Luis, *J. Adv. Oxid. Tech.*, **11**, 11 (2008).
9. A. Menendez, J. I. Lombrana and A. de Luis, *J. Adv. Oxid. Tech.*, **11**, 573 (2008).
10. APHA, AWW, WEF, *Standard methods for the examination of water and waste water*, 19th Ed; American Public Health Association/ American Water Works Association/Water Environment Federation, Washington, DC (1995).
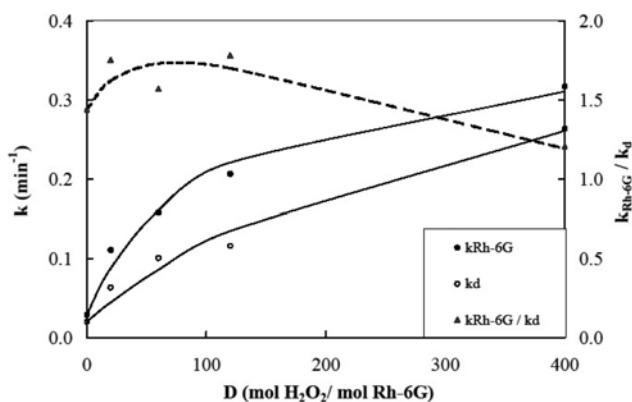11. H. W. Chen, Y. L. Kuo, C. S. Chiouc, S. W. You, C. M. Ma and C. T.

Fig. 11. Kinetic comparison of both processes: Rh-6G removal and decoloration at pH 3.

Chang, *J. Hazard. Mater.*, **174**, 795 (2010).

12. E. Kusvuran, O. Gulnaz, S. Irmak, O. M. Atanur, H. I. Yavuz and O. Erbatur, *J. Hazard. Mater.*, B**109**, 85 (2004).

13. C. H. Wua and C. L. Chang, *J. Hazard. Mater.*, **B128**, 265 (2006).

14. M. A. Behnajady, N. Modirshahla and H. Fathi, *J. Hazard. Mater.*, **B136**, 816 (2006).

15. A. Aleboyeh, H. Aleboyeh and Y. Moussa, *Dyes Pigments*, **57**, 67 (2003).

16. B. Gozmen, B. Kayan, A. M. Gizir and A. Hesenov, *J. Hazard. Mater.*, **168**, 129 (2009).

17. O. L. C. Guimaraes, D. N. V. Filho, A. F. Siqueira, H. J. I. Filho and M. B. Silva, *Chem. Eng. J.*, **141**, 35 (2008).

18. R. W. Gaikwad and S. A. M. Kinldy, *Korean J. Chem. Eng.*, **26**(1), 102 (2009).

19. T. M. Elmorsi, Y. M. Riyad, Z. H. Mohamed and H. M. H. Abd El Bary, *J. Hazard. Mater.*, **174**, 352 (2010).

20. K. Belkacemi, F. Larachi and A. Sayari, *J. Catal.*, **193**, 224 (2000).

21. E. B. Azevedo, F. R. de Aquino Neto and M. Dezotti, *J. Hazard. Mater.*, **B128**, 182 (2006).

22. W. Chu and C. W. Ma, *Chemosphere*, **37**, 961 (1998).

23. I. Arslan and A. I. Balcioglu, *J. Chem. Technol. Biot.*, **76**, 53 (2001).

24. R. A. Mansoori, S. Kothari and R. Ameta, *Arab. J. Sci. Eng.*, **29**(1A), 11 (2004).

25. J. C. Crittenden, S. Hu, D. W. Hand and S. A. Green, *Water Res.*, **33**(19), 2315 (1999).

26. H. Y. Shu, M. C. Chang and W. P. Hsieh, *J. Hazard. Mater.*, **B128**, 60 (2006).

27. F. H. AlHamedi, M. A. Rauf and S. S. Ashraf, *Desalination*, **239** (1-3), 159 (2009).

28. B. Xu, N. Y. Gao, H. Cheng, S. J. Xia, M. Rui and D. D. Zhao, *J. Hazard. Mater.*, **162**, 954 (2009).

29. A. de Luis, J. I. Lombraña, F. Varona and A. Menéndez, *Korean J. Chem. Eng.*, **26**(1), 48 (2009).